LA-8141-MS

Informal Report

2

A Model of Burning and Detonation in Rocket Motors

LOS ALAMOS SCIENTIFIC LABORATORY

Post Office Box 1663 Los Alamos, New Mexico 87545

This report was not edited by the Technical Information staff.

UNITED STATES
DEPARTMENT OF ENERGY
CONTRACT W-7405-ENG. 36

LA-8141-MS
Informal Report
UC-33
Issued: January 1980

A Model of Burning and Detonation in Rocket Motors

Charles A. Forest

A MODEL OF BURNING AND DETONATION IN ROCKET MOTORS

by

Charles A. Forest

ABSTRACT

Rocket motor dome failure may produce a damaged porous bed of propellant adjacent to the motor case. This porous bed of propellant may burn and ultimately cause detonation of the motor. A numerical model is presented which examines detonation of the solid propellant grain from shocks induced by the burning porous bed. Calculations are made in one- and two-dimensional cylindrical geometry and employ the Forest Fire model of shock-induced decomposition.

I. INTRODUCTION

Motor detonations have occurred in some full-scale experimental rocket motors. In particular, second-stage test motors have detonated following motor dome rupture. Various scenarios have been proposed to explain this catastrophic event. One such scenario is the "shear" scenario in which, following dome failure, the motor case moves with respect to the motor grain, creating a porous bed of shear-damaged propellant next to the case. The damaged propellant bed is confined by the motor case and remaining solid propellant. With sufficient burning surface, the damaged porous bed becomes a region in which deflagration-to-detonation transition (DDT) may occur. Detonation may occur in the damaged propellant or in the solid propellant interior to the damaged propellant.

The calculations presented here examine the scenario in which the burning damaged bed does not undergo detonation, but rather sends pressure waves into the solid which ultimately build to shocks and cause initiation of detonation in the solid propellant. Numerical modeling is made with the full-scale motor dimensions in one-dimensional cylindrical (R) and two-dimensional cylindrical (R,Z) geometries, where R = radial position and Z = axial position.

II. ONE-DIMENSIONAL CALCULATIONS

A. The Model

The one-dimensional cylindrical geometry calculations were made with the SIN hydrodynamics code.[1,2] The problem geometries are listed in Table I, with

TABLE I

ONE-DIMENSIONAL CYLINDRICAL PROBLEM GEOMETRY

Region	Material	Density (g/cm^3)	Total Thickness (cm)			Cells Number/Length (cm)		
Motor bore	VOP 7 products	0.028	37.59			60/0.6265		
Propellant grain[a]	VOP 7 solid, normal density	1.91	54.25	52.75	50.25	217/0.25	211/0.25	201/0.25
Porous propellant bed[a]	VOP 7 solid, 0.9 x normal density	1.719	1.0	2.6	5.0	5/0.20	13/0.20	25/0.20
Motor case	Kevlar	1.412	1.4			14/0.10		
Exterior to motor	Air	0.00107	4.0			10/0.40		

[a]Three thicknesses are given for the porous bed region with corresponding solid grain thicknesses.

the innermost material regions listed first and then proceeding down the list to the outer regions.

About the cylindrical axis is the motor bore which is filled with VOP 7* decomposition products at an initial pressure of 0.0001 Mbar. Surrounding the bore is the solid propellant grain, also at 0.0001-Mbar initial pressure, with shock-induced decomposition allowed by the Forest Fire[3,4] model. Next is the damaged VOP 7 propellant porous bed. The porous bed is taken to be composed of uniformly shaped particles with a specified initial surface-to-volume ratio. The initial pressure is 0.0005 Mbar, obtained by setting the mass fraction of propellant burned to 0.002. Burning of the particles is modeled by the "porous bed burn" model, which assumes laminar burning on the surfaces of the particles. (See "Bulk Burn" in Ref. 4.) The surface-to-volume ratio and thickness of the porous bed region is varied to examine the sensitivity of the computed outcome (for instance, partial decomposition or detonation in the solid propellant grain) to these variables. Confining the porous bed from the outside is the motor case which is made of Kevlar. Kevlar has material strength with shear modulus μ = 0.172 and yield strength Y_0 = 0.01034 Mbar. Air surrounds the motor case.

The HOM[1] equation of state is used throughout. HOM represents solid materials by a Grüneisen expansion off the first shock Hugoniot, gases by a Beta-law expansion off a BKW-computed[5] isentrope, and mixtures of solid and gases by assuming pressure and temperature equilibrium. HOM constants for each material are given in Table II.

The Forest Fire shock-induced explosive decomposition model is the decomposition rate necessary to accelerate a shock wave along the "Pop-Plot" curve. (The Pop-Plot is the graph of distance to detonation as a function of initial shock pressure and is named for Alphonse Popolato, its originator).[6] Included in the Forest Fire analysis is a method of estimating the Pop-Plot shifts and corresponding reaction rate changes due to a change in the initial explosive density. Figure 1 shows the experimental Pop-Plot for VOP 7[7] at density ρ_0 = 1.91 (g/cm^3) and the computed Pop-Plot at density ρ_0 = 1.719 (g/cm^3). Figure 2

*VOP 7 is an obsolete HMX-based experimental propellant.

TABLE II

```
 VOP-7, RHO=1.91

UNREACTED SOLID, HOM CONSTANTS
+0.2                +3.6                +0.478445           +0.243
+1.879              -1.35733168580E+01-8.64978401037E+01-1.42462911036E+02
-9.99233449144E+01-2.35377505339E+01+1.5                    +0.33
+5.23560209424E-01+0.00012              +0.                 +0.
+300.               +0.                 +0.                 +0.
+0.                 +0.                 +0.478445
DETONATION PRODUCTS, HOM CONSTANTS
-3.59225007104E+00-2.25139095825E+00+3.07083271071E-01-3.38388105816E-02
+3.26317134386E-04-1.56957579961E+00+5.63240444420E-01+9.14476859528E-02
+8.61048912339E-03+3.20340178818E-04+8.05038175417E+00-4.75298681101E-01
+1.00767476473E-01+5.25836857192E-03-4.21628859215E-03+0.5
+0.1


 VOP-7   RHO=1.7190 = 0.90*1.91,  GRUNEISEN FIT FOR SOLID, BKW GAS

UNREACTED SOLID, HOM CONSTANTS
+0.058              +4.4                +0.485693           +0.12737
+2.418              +5.35308101554E+01+2.80424429325E+02+6.10873944231E+02
+5.87554896556E+02+2.12269894127E+02+1.5                    +0.33
+5.81733566027E-01+0.00012              +0.                 +0.
+300.               +0.                 +0.                 +0.
+0.                 +0.                 +0.485693
DETONATION PRODUCTS, HOM CONSTANTS
-3.48829964362E+00-2.21293918558E+00+2.84088396236E-01-3.45908309471E-02
+1.61341661461E-03-1.52769658343E+00+5.11751877215E-01+6.91391026790E-02
+5.09642892264E-03+1.40021106127E-04+8.14735025976E+00-4.29018154047E-01
+8.86488937040E-02-1.18036109477E-02+6.09785049038E-04+0.5
+0.1


 KEVLAR

SOLID, HOM CONSTANTS
+0.4                +1.5                +0.                 +0.
+0.                 +0.                 +0.                 +0.
+0.                 +0.                 +1.5                +0.3
+0.708215298       +4.0          E-05+0.                   +0.
+300.               +1.0          E-06+0.006897           +0.172
+0.050              +0.                 +0.


 AIR

DUMMY SOLID, HOM CONSTANTS
+0.0
+0.0
+0.0
+929.6531464
+300.               +0.00001
+0.0
BKW GAS, HOM CONSTANTS
-2.36733372864+000-1.23356432554+000+2.15170143603-002-2.95528542190-003
+1.22549782445-004-5.53376189904-001+2.44880013455-003-1.80516553555-002
-1.21968671688-003-2.53726183472-005+9.88588851357+000-2.35014643148-001
+3.36987666054-002-4.21156020156-003+1.63045512702-004+0.5
+0.1
```

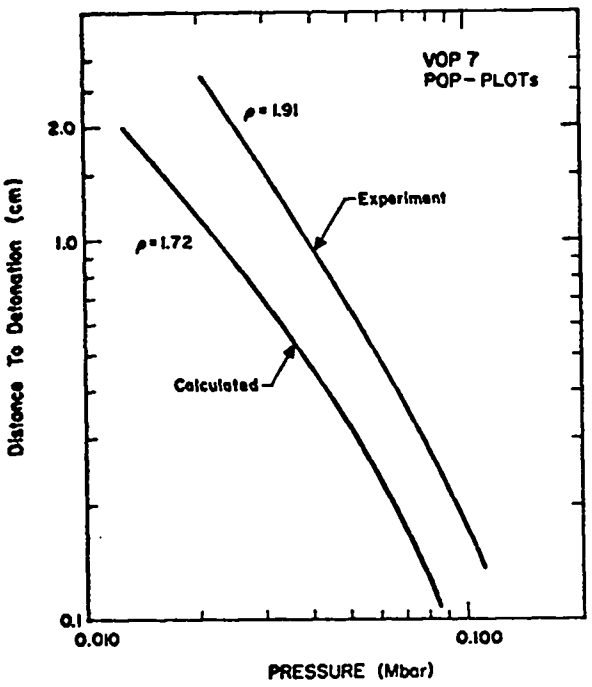

Fig. 1.
Distance to detonation as a function of initial shock pressure. The experimental line is from LASL Group M-3 wedge test data. The $\rho_0 = 1.72$ line is calculated using the $\rho_0 = 1.91$ data.

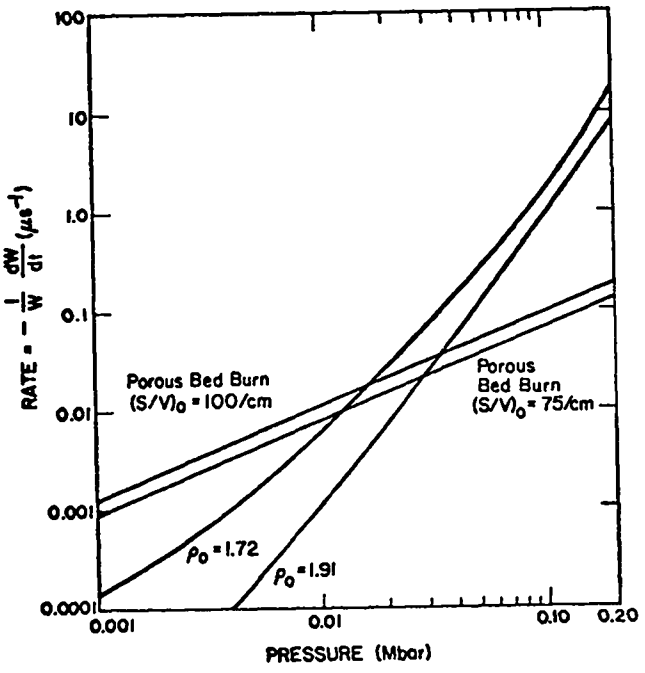

Fig. 2.
Forest Fire and porous bed burn decomposition rates. The two curves $\rho_0 = 1.91$ and $\rho_0 = 1.72$ are Forest Fire rates based on the Pop-Plot of Fig. 1. The porous bed burn rates are the initial W = 1 rates.

shows the Forest Fire decomposition rates for the two densities. A listing of the computed rates as well as the polynomial fit is given in the appendix.

The porous bed burn model assumes uniform particles burning on their surfaces. The burning surface is also assumed to move normal to the surface at the linear burning velocity, $dx/dt = kP^n$. In particular, it is assumed that the surface area is constant; that is, the propellant is sheared into sheets. The time derivative of mass fraction, dW/dt, (μs^{-1}) is then

$$dW/dt = -(S/V)_0 \, kP^n \quad ,$$

with

$(S/V)_0$ = initial surface-to-volume ratio,

$k = +0.00617785$,

$n = +0.911$,

and with P in megabars. Figure 2 shows the decomposition rate as a function of pressure for $(S/V)_0 = 75/cm$ and 100/cm. The entire region is assumed to be ignited and burning at time $t = 0$.

B. Calculated Results

The thickness of the damaged bed and the initial surface-to-volume ratio $(S/V)_0$ are varied. The figure numbers, the initial conditions, and time to detonation (t_{det}) of the various calculations are listed in Table III.

In each of Figs. 3a-5 is shown a sequence of frames. Each frame shows a plot of mass fraction of unreacted propellant and pressure as a function of distance for a given time. The mass fraction scale is always 0. to 1. with 1. being all unreacted propellant. The pressure scale is noted at the lower right corner (for example, 50 kbar) and changes to 400 kbar when the maximum pressure exceeds 50 kbar. Time indicated is in microseconds.

Cylindrical convergence adds some to the pressure increase as the pressure waves move inward. However, since the center bore is a large fraction of the outer radius, the effect of cylindrical convergences is limited. Principally, the occurrence of detonation is determined by the balance between the burning in the porous region, which forms pressure waves into the solid, and the case movement, which relieves the pressure. The shock sensitivity of the adjacent solid determines the response to the imposed pressure waves.

III. TWO-DIMENSIONAL CALCULATIONS

A. The Model

The two-dimensional calculations were made with the 2DL code, which is a two-dimensional, Lagrangian, finite difference computer program operable in (x,y) slab geometry or (R,Z) cylindrical geometry. The calculations presented here are in two-dimensional (R,Z) cylindrical geometry where R = radial position and Z = axial position. The problem geometry is shown in Fig. 6. Here the (R,Z) space is defined by regions, which are further subdivided into cells as shown.

TABLE III

ONE-DIMENSIONAL CYLINDRICAL CALCULATIONS

Figure Number	Bed Thickness (cm)	$(S/V)_0$ [a] (1/cm)	t_{det} (μs)
3a	5.0	40	171.9
3b	5.0	80	29.5
3c	5.0	120	21.1
4a	2.6	40	no det.
4b	2.6	80	75.1
4c	2.6	120	25.3
5	1.0	80	no det.

[a] A 1-mm cube has S/V = 60/cm.

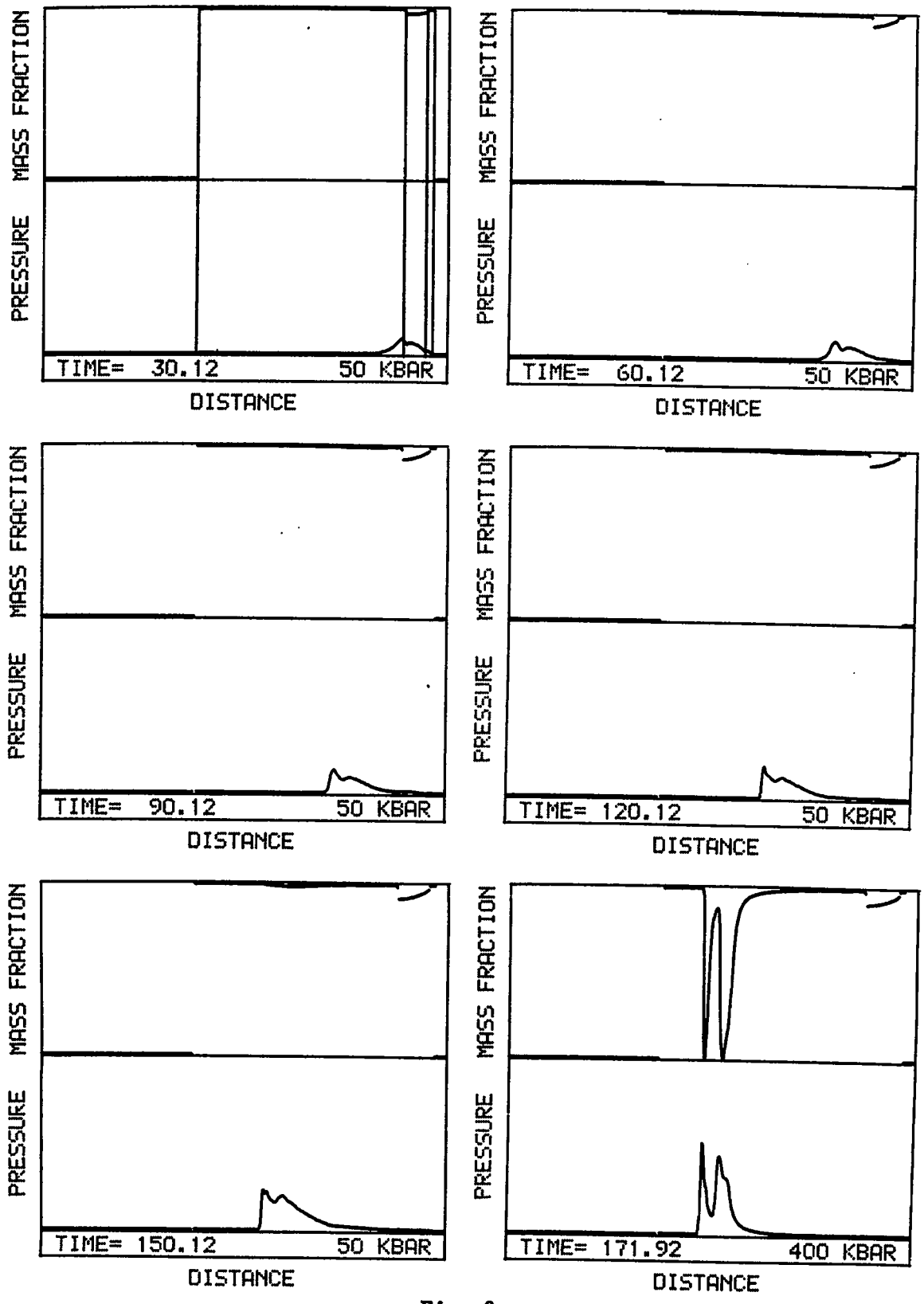

Fig. 3a.
One-dimensional cylindrically symmetric calculation with a 5-cm-thick porous bed and with $(S/V)_0$ = 40/cm.

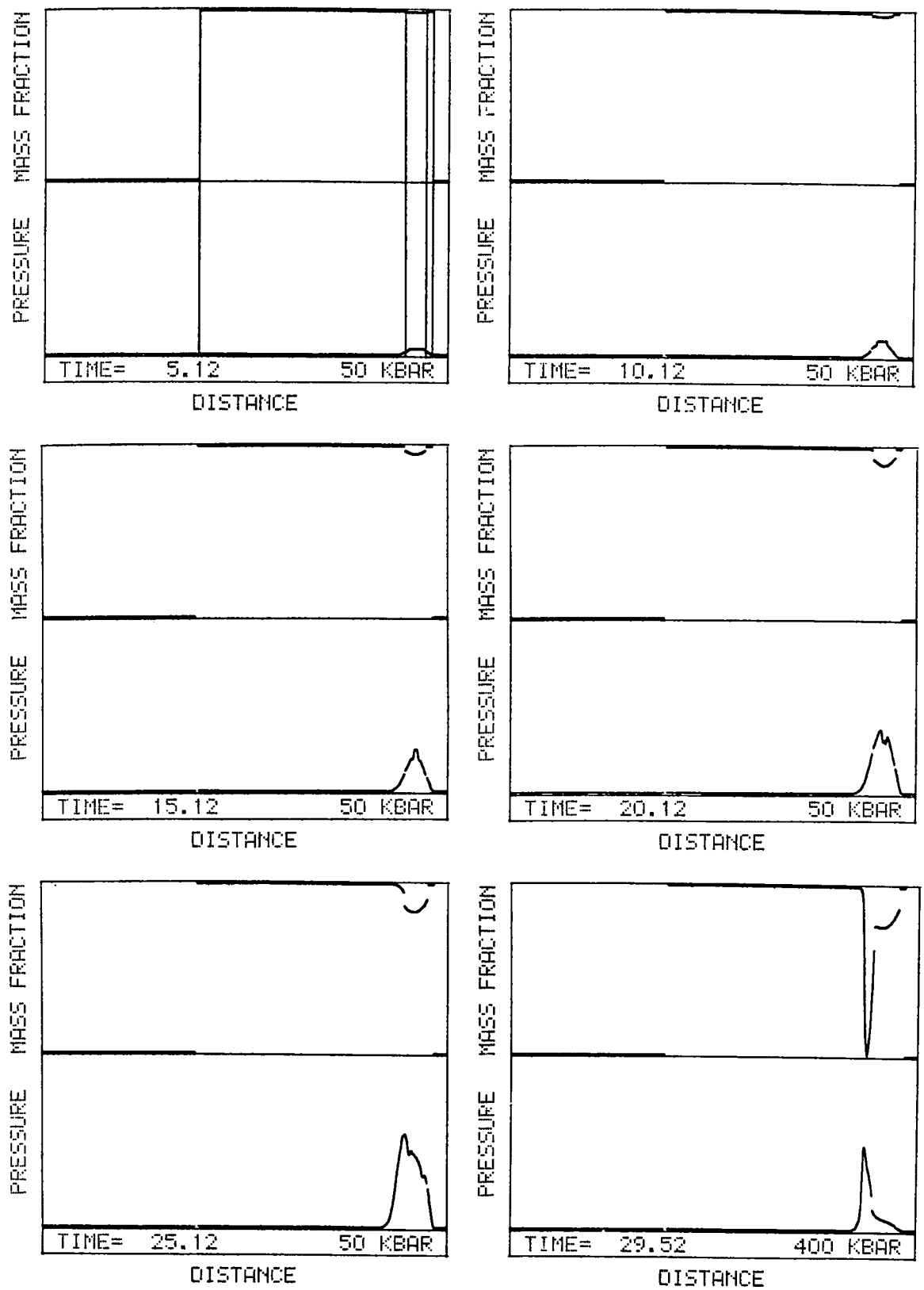

Fig. 3b.
One-dimensional cylindrically symmetric calculation with a 5-cm-thick porous bed and with $(S/V)_0$ = 80/cm.

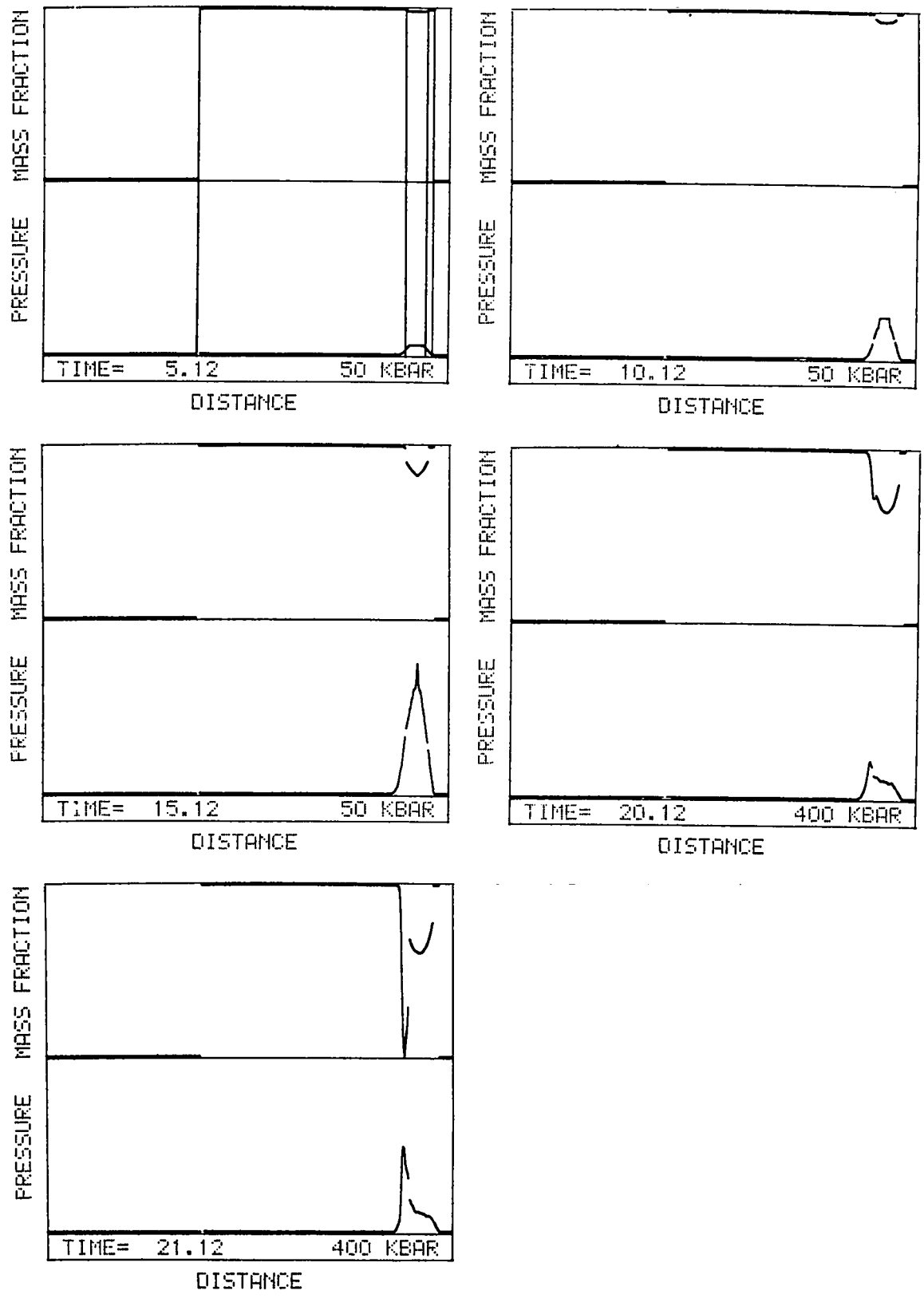

Fig. 3c.
One-dimensional cylindrically symmetric calculation with a 5-cm-thick porous bed and with $(S/V)_0$ = 120/cm.

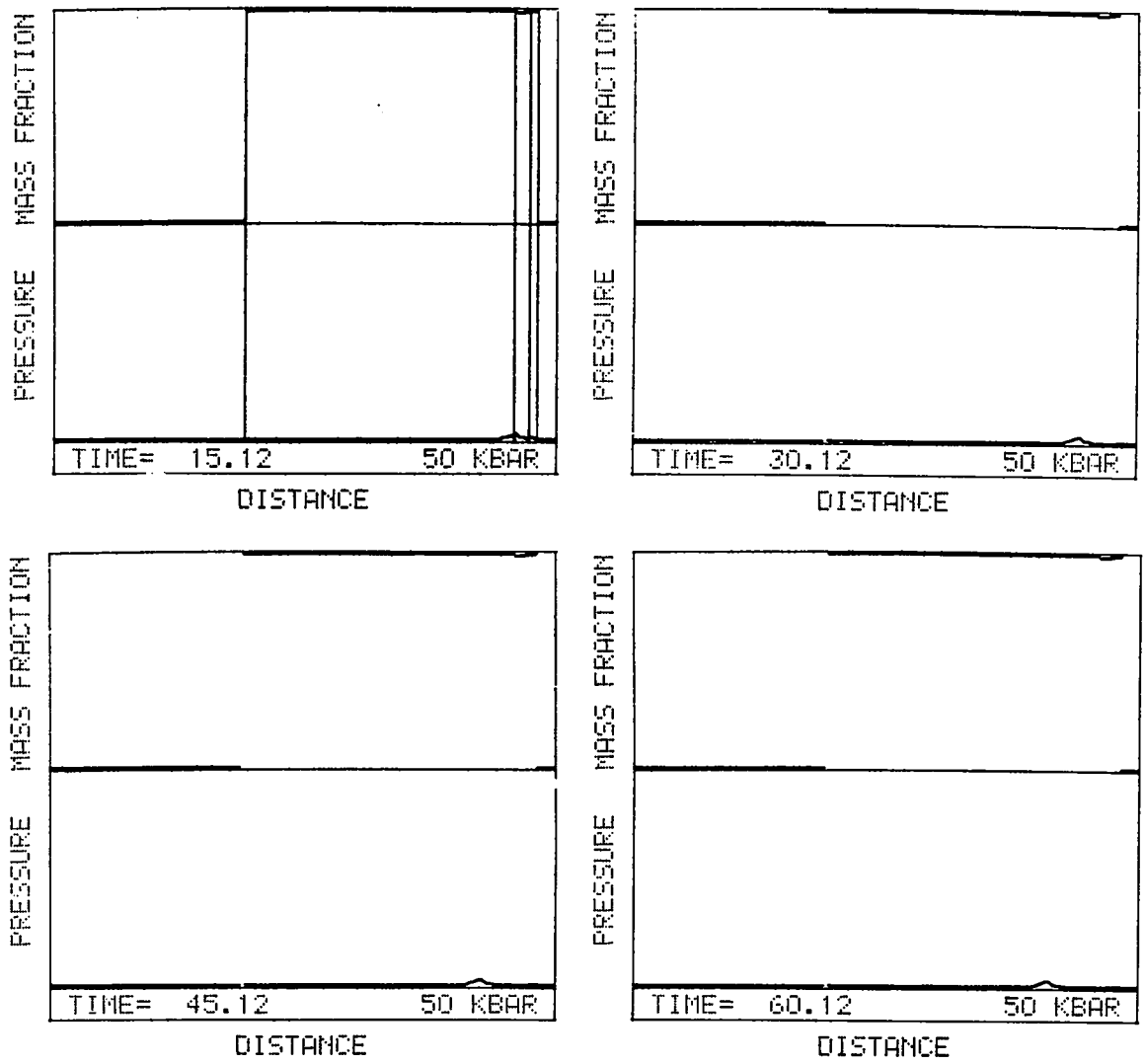

Fig. 4a.
One-dimensional cylindrically symmetric calculation with a 2.6-cm-thick porous bed and with $(S/V)_0$ = 40/cm.

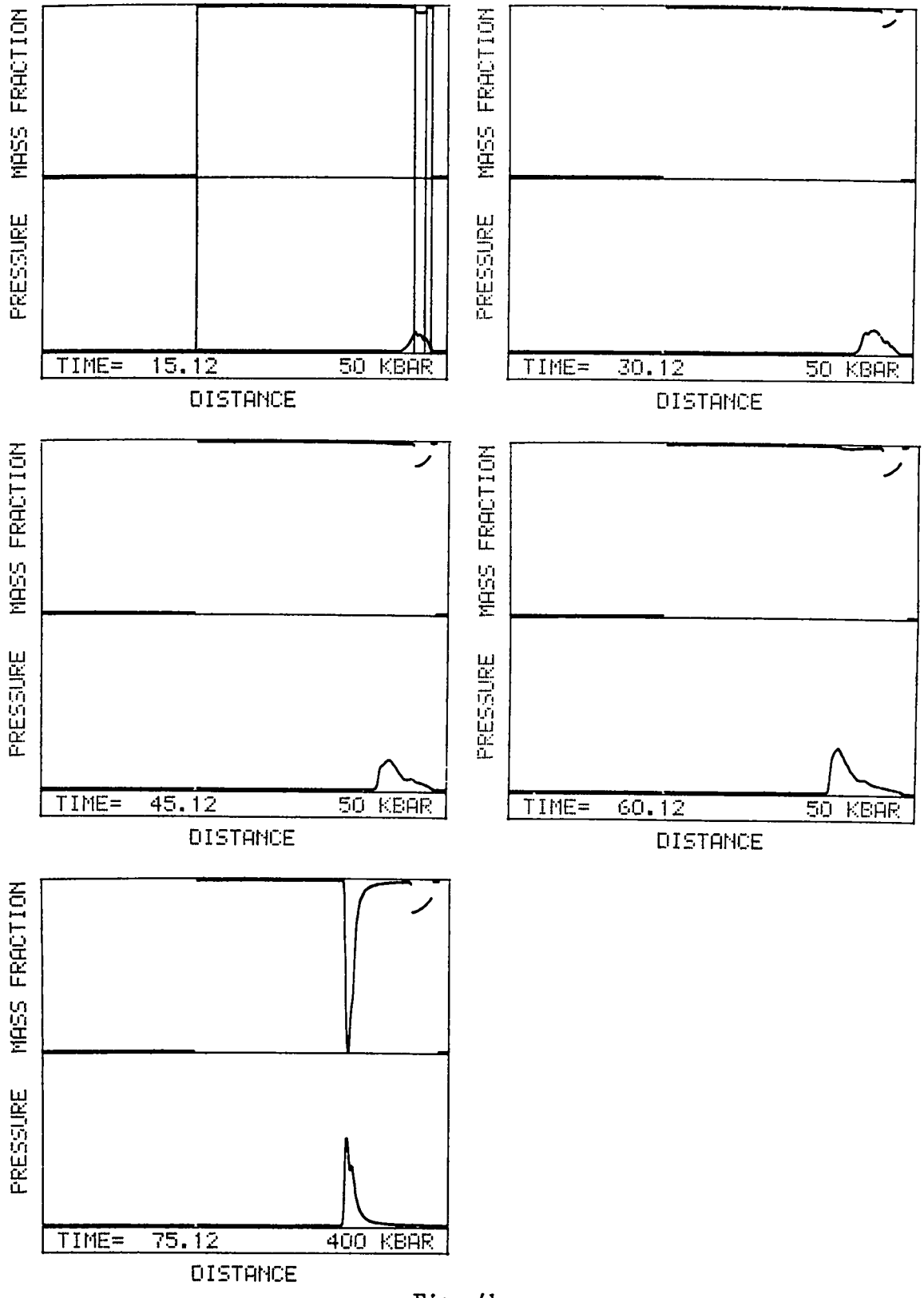

Fig. 4b.
One-dimensional cylindrically symmetric calculation with a 2.6-cm-thick porous bed and with $(S/V)_0$ = 80/cm.

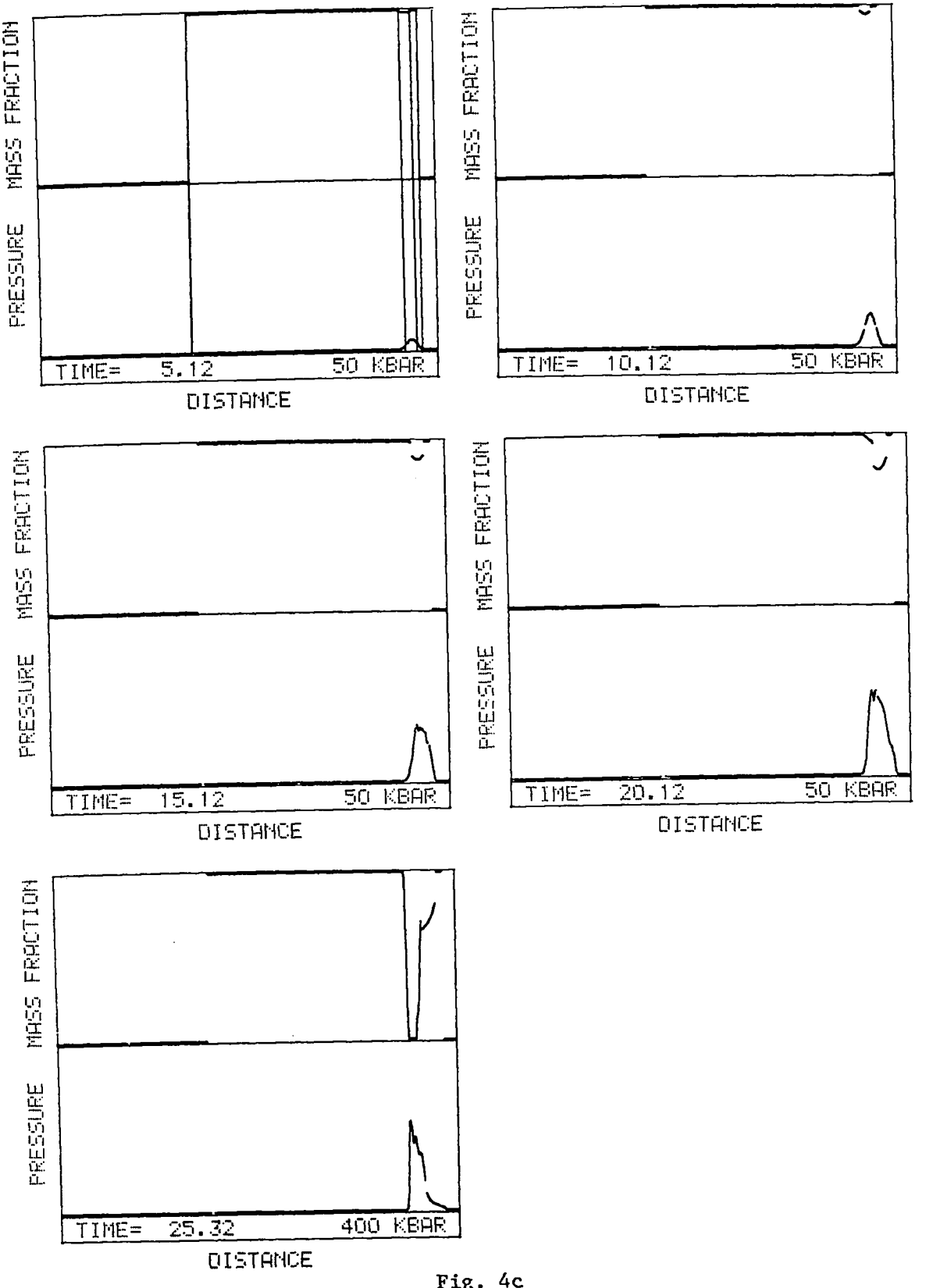

Fig. 4c
One-dimensional cylindrically symmetric calculation with a 2.6-cm-thick porous bed and with $(S/V)_0$ = 120/cm.

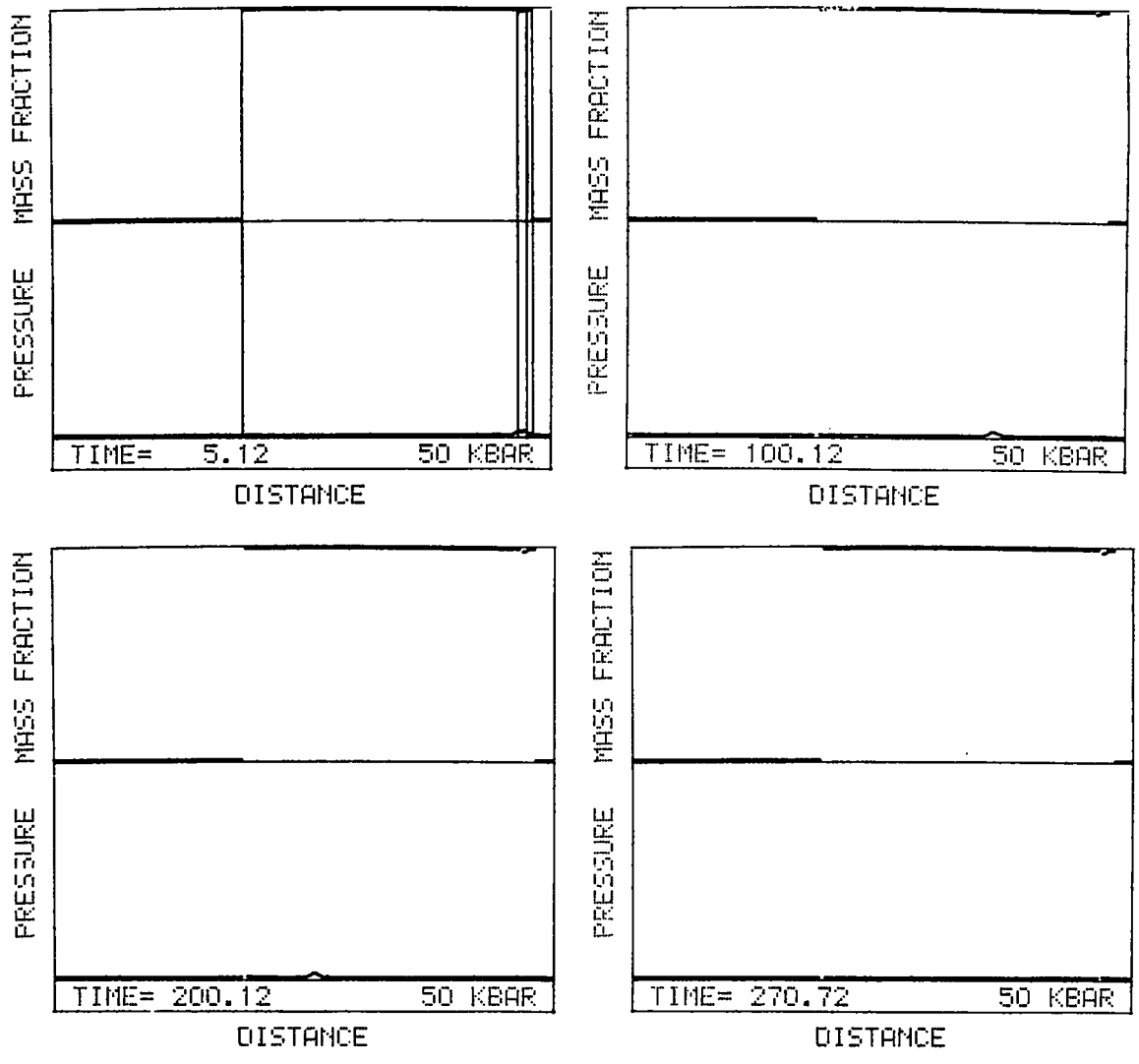

Fig. 5.
One-dimensional cylindrically symmetric calculation with a 1.0-cm-thick porous bed and with (S/V) = 80/cm.

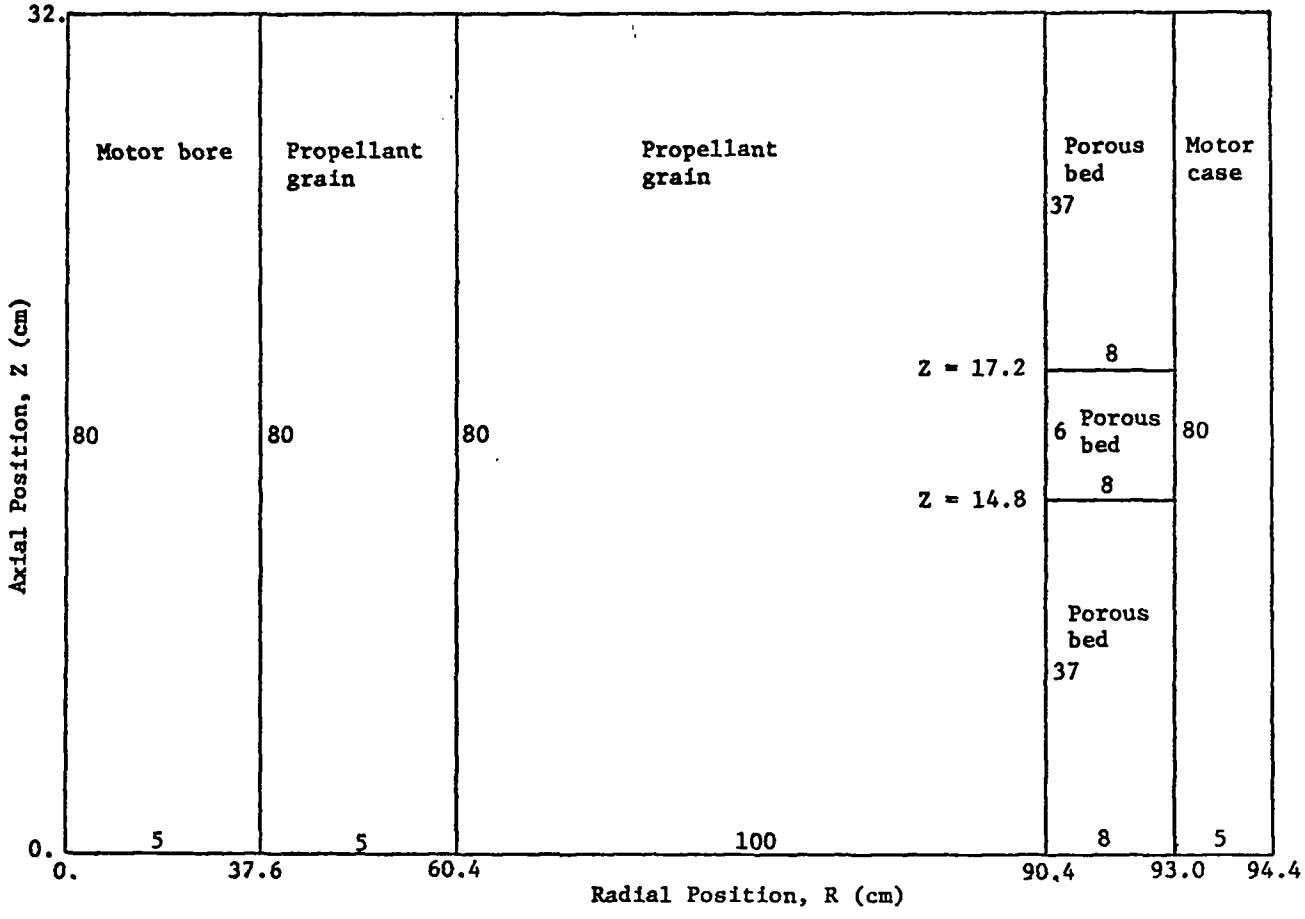

Fig. 6.
Schematic of two-dimensional cylindrical problem geometry (not to scale). The numbers interior to the regions indicate the number of cell divisions for that side. The small region of porous bed is the region of initial ignition for the case of a 2.4-cm segment. The region is two cells high for the case of a 0.8-cm initial ignition segment.

Since the leftmost regions do not enter the calculation during the time of interest, the motor bore and adjacent solid propellant grain are "filled in" with large radial cells. The principal region of interest (the outer part of the solid grain, the 2.6-cm-thick porous bed, and the motor case) is partitioned into much smaller cells. The small region in the vertical center of the porous bed shell is the region assumed to be initially ignited; that is, burning by the porous bed burn model. The ignition is spread from this initial ignition segment of the porous bed shell into the adjacent porous bed at a velocity of 0.1 cm/μs in both upward and downward directions. Note that, because of the geometric rotational symmetry, each region is a cylindrical shell segment and the region of initial ignition is thus a ring. The ignition mechanism is not under consideration here; hovever, one possibility for such ignition is flame penetration into a grain fracture that radiates from the bore to the motor case.

The motor case has strength as in the one-dimensional situation. The outer surface of the case is defined to be a free surface (a 2DL boundary option); the

air that surrounded the case in the one-dimensional calculations is not present in the two-dimensional calculation.

The HOM equation of state, the porous bed burn, and the Forest Fire rate constants are as previously specified in the one-dimensional problems.

B. Calculated Results

The length of the initial ignition segment and the initial surface-to-volume ratio are varied. Listed in Table IV, for each calculation, are the figure number, the initial ignition segment length, the initial surface-to-volume ratio, and the time to detonation if detonation occurred during the span of the calculation. If detonation did not occur by the end of the computer run, times and associated maximum pressures near the end of the computer run are listed to indicate the progress of the calculation at those times.

Figures 7a-8d show pressure contours for the region near the motor case in a sequence of frames at various times. The inner radius in each frame is 60.4 cm; the outer radius is 100.0 cm. The vertical (axial) interval is 0.-32.0 cm, which encompasses the fine partitioned regions of the calculation. The region beyond the outer surface of the motor case, which is defined as a free surface, is to be considered as a void. The time on each frame is in microseconds and is the elapsed time from the onset of burning of the porous bed. P MAX refers to maximum pressure and is in kilobars. P INTV refers to the contour spacing for pressure and is also in kilobar units. The contour interval spacing changes to limit the number of contour lines drawn.

TABLE IV

TWO-DIMENSIONAL CYLINDRICAL CALCULATIONS

Figure	Initial Ignition (cm)	$(S/V)_0$ (cm^{-1})	Time to Detonation (μs)	Condition at End of Calculation	
				Time (μs)	Pressure (kbar)
7a	0.8	125		50.0	12.9
				52.2	11.3
7b	0.8	150		50.0	36.1
				50.3	38.7
7c	0.8	175	36.1		
8a	2.4	100		40.0	9.8
				42.0	10.4
8b	2.4	125		50.0	15.9
				58.6	25.6
8c	2.4	150	32.9		
8d	2.4	175	24.7		

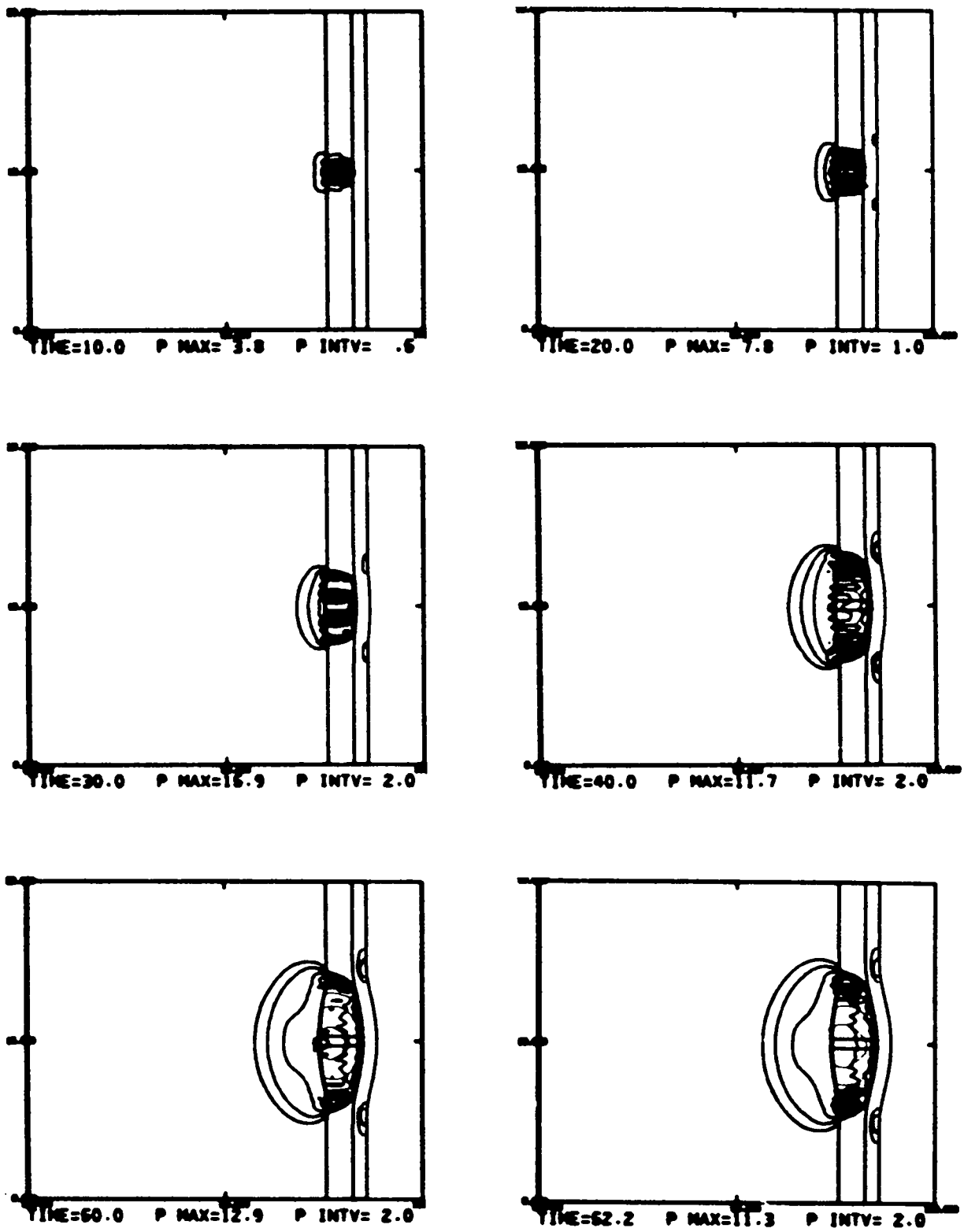

Fig. 7a.
Calculated 2DL pressure contours with two-dimensional cylindrical (R,Z) geometry in the region $60.4 \leq R \leq 100$ and $0 \leq Z \leq 32$. The initial ignition segment is 0.8 cm and $(S/V)_0 = 125/cm$ in the porous bed.

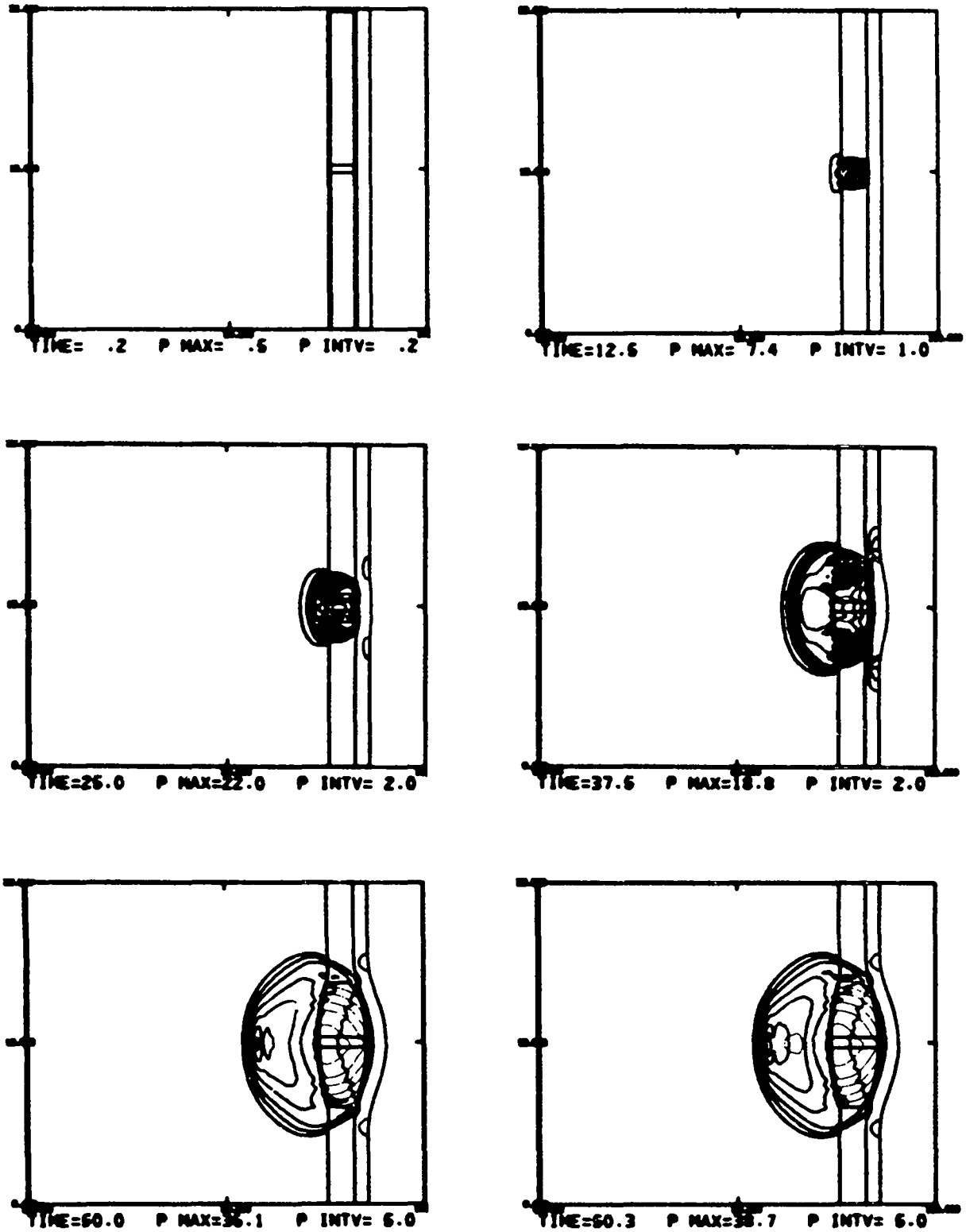

Fig. 7b.
Calculated 2DL pressure contours with two-dimensional cylindrical (R,Z) geometry in the region $60.4 \leq R \leq 100$ and $0 \leq Z \leq 32$. The initial ignition segment is 0.8 cm and $(S/V)_0$ = 150/cm in the porous bed.

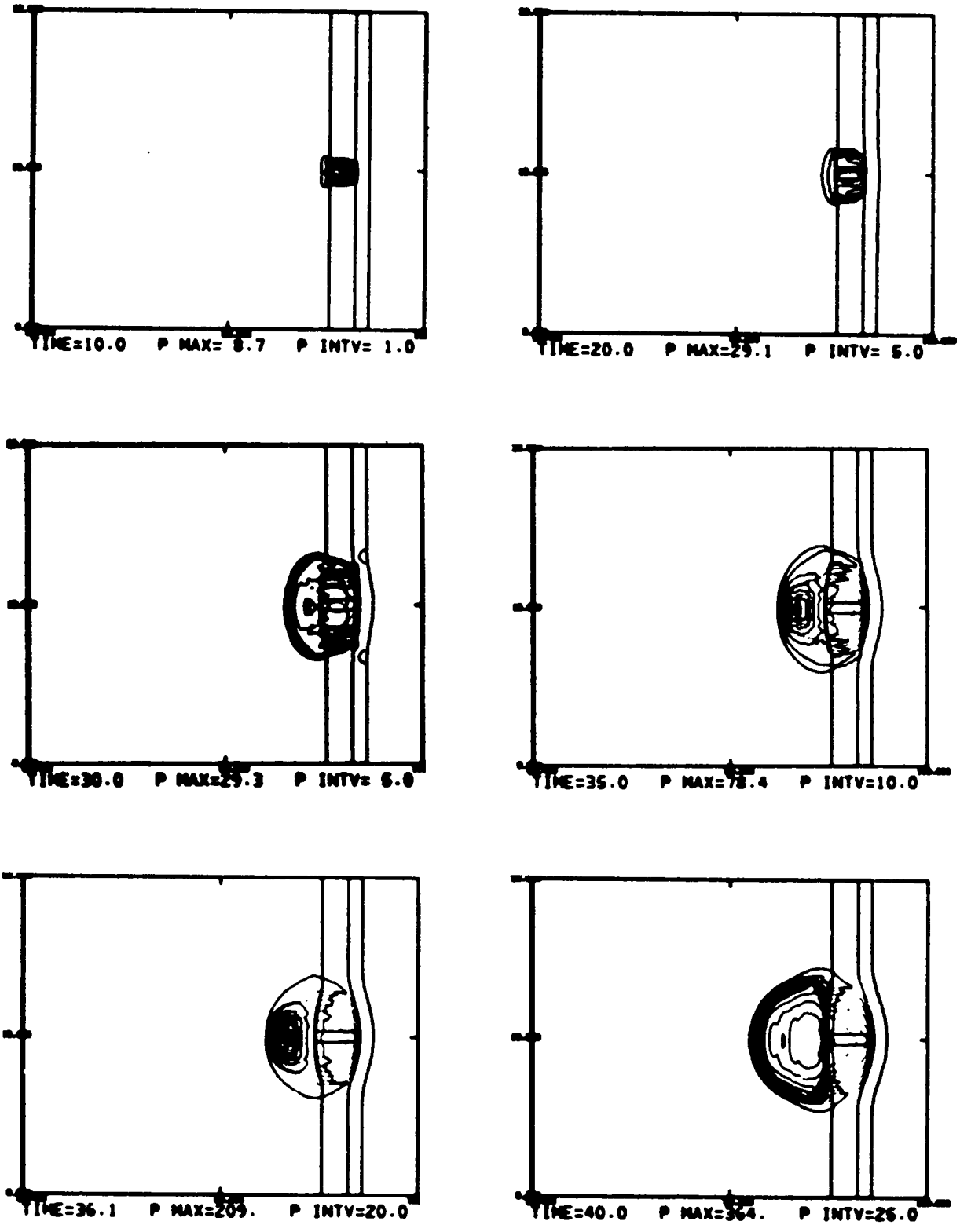

Fig. 7c.
Calculated 2DL pressure contours with two-dimensional cylindrical (R,Z) geometry in the region $60.4 \leqslant R \leqslant 100$ and $0 \leqslant Z \leqslant 32$. The initial ignition segment is 0.8 cm and $(S/V)_0 = 175/cm$ in the porous bed.

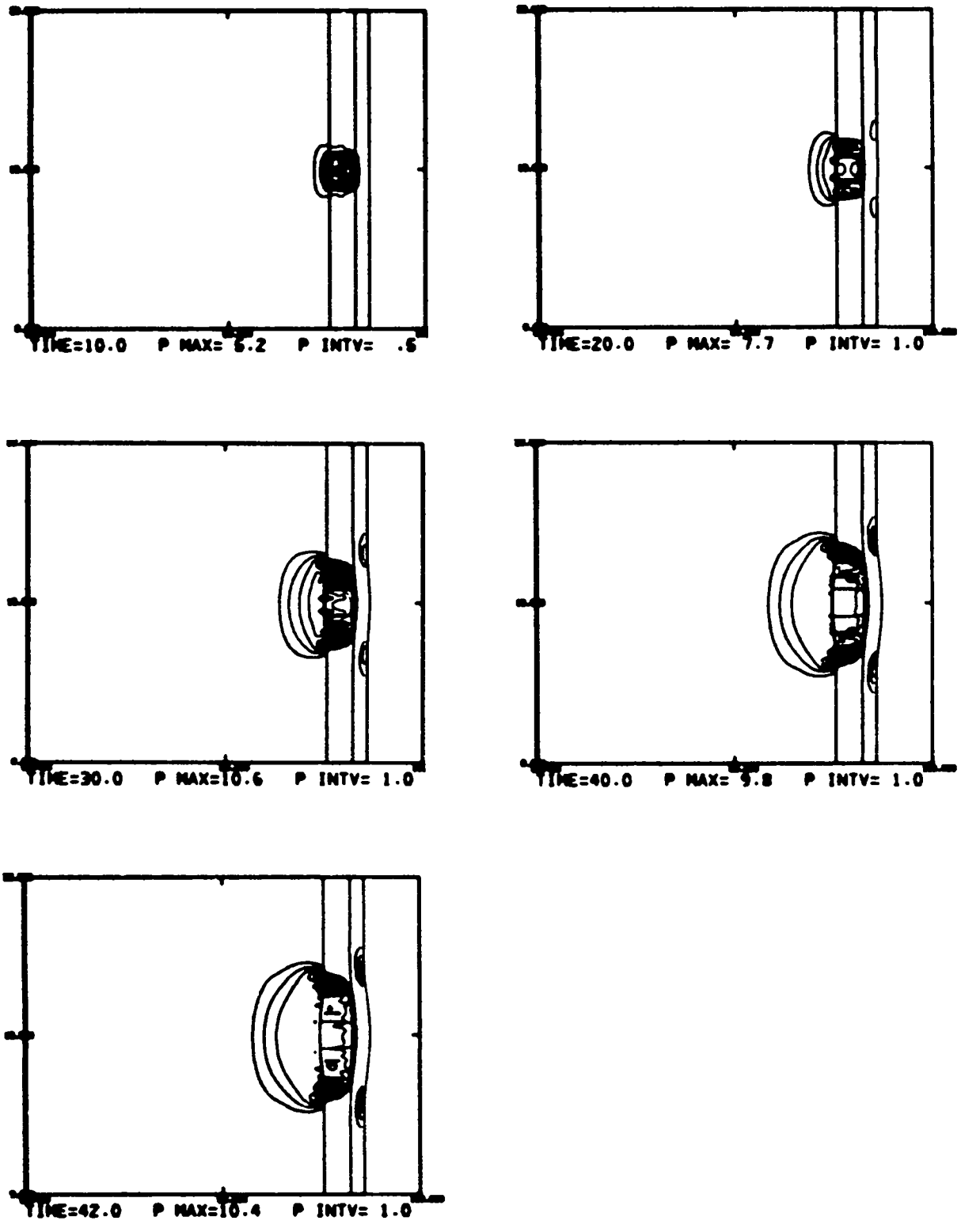

Fig. 8a.
Calculated 2DL pressure contours with two-dimensional cylindrical (R,Z) geometry in the region $60.4 \leq R \leq 100$ and $0 \leq Z \leq 32$. The initial ignition segment is 2.4 cm and $(S/V)_0 = 100/cm$ in the porous bed.

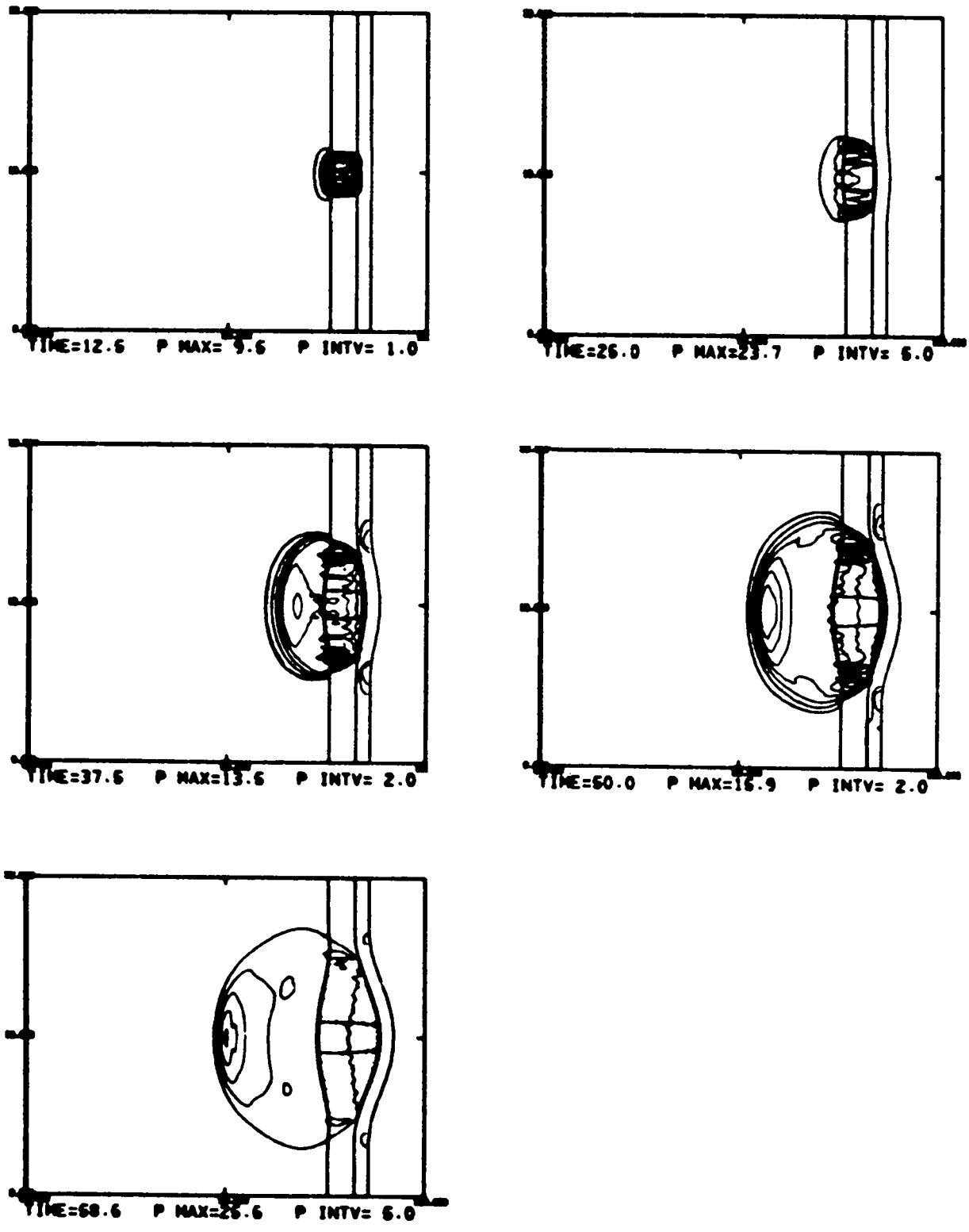

Fig. 8b
Calculated 2DL pressure contours with two-dimensional cylindrical (R,Z) geometry in the region $60.4 \leqslant R \leqslant 100$ and $0 \leqslant Z \leqslant 32$. The initial ignition segment is 2.4 cm and $(S/V)_0 = 125/cm$ in the porous bed.

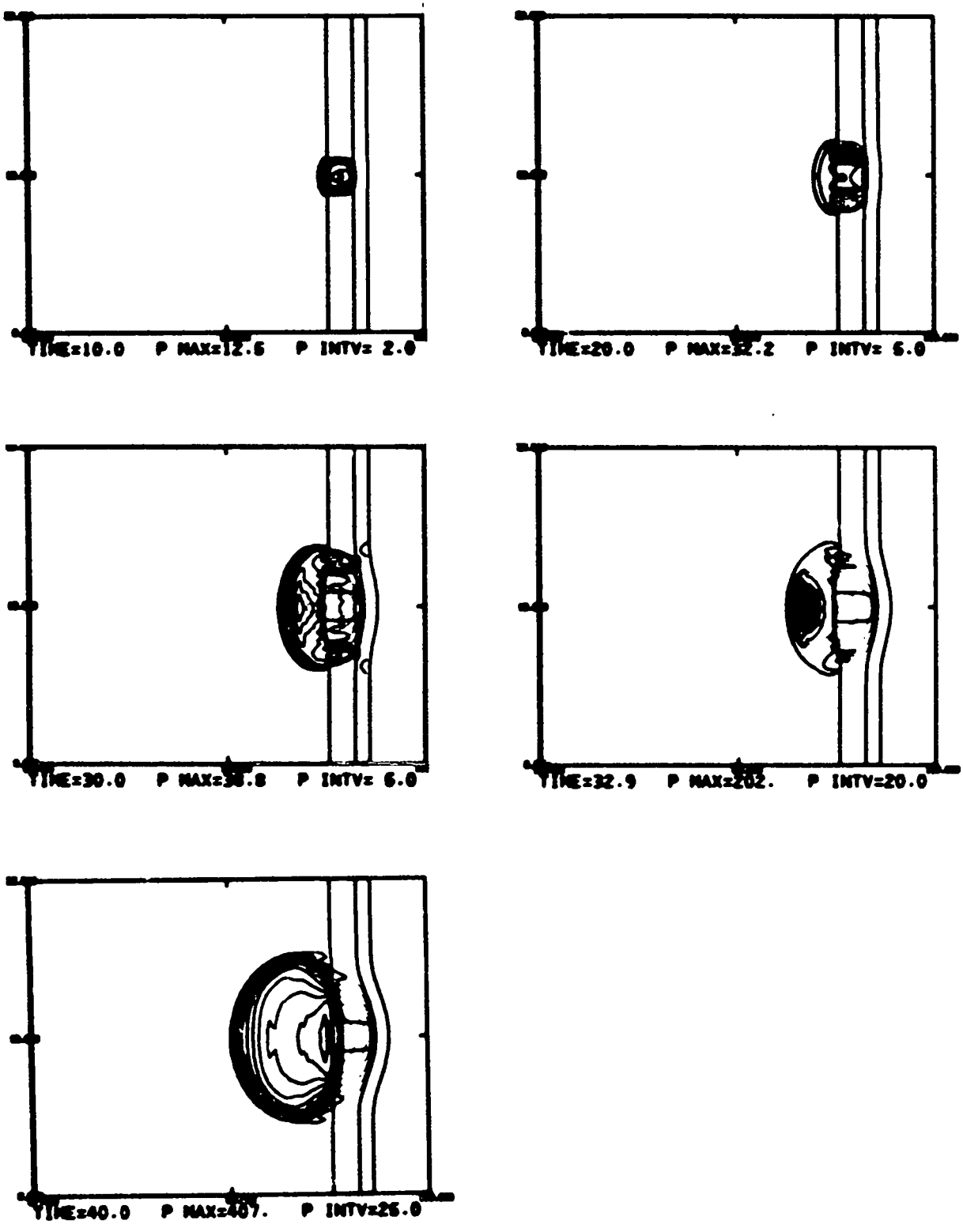

Fig. 8c.
Calculated 2DL pressure contours with two-dimensional cylindrical (R,Z) geometry in the region $60.4 \leq R \leq 100$ and $0 \leq Z \leq 32$. The initial ignition segment is 2.4 cm and $(S/V)_0$ = 150/cm in the porous bed.

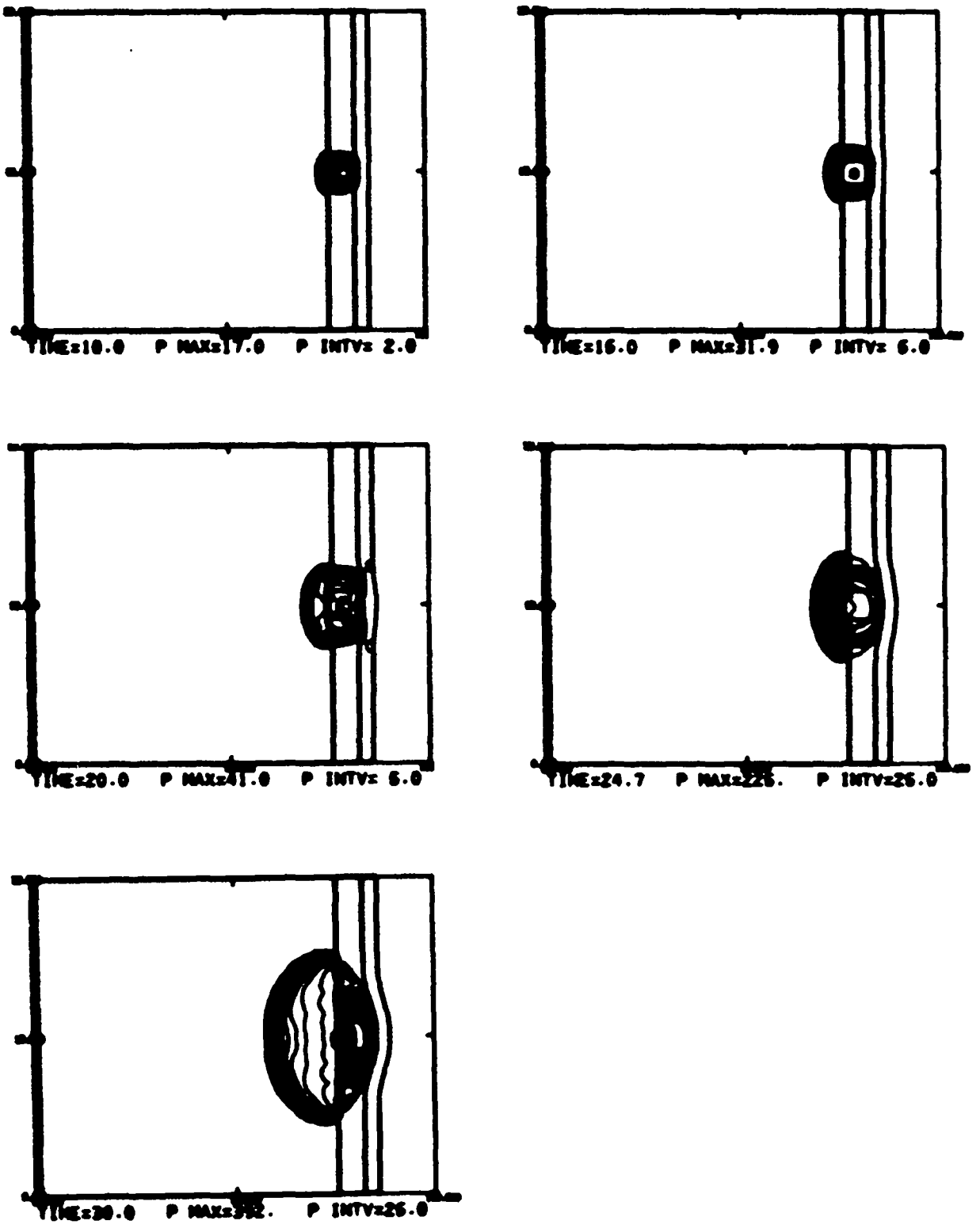

Fig. 8d.
Calculated 2DL pressure contours with two-dimensional cylindrical (R,Z) geometry in the region $60.4 \leq R \leq 100$ and $0 \leq Z \leq 32$. The initial ignition segment is 2.4 cm and $(S/V)_0 = 175/cm$ in the porous bed.

IV. CONCLUSIONS

In the one-dimensional SIN calculations, Figs. 3a-5, fairly modest (40 to 120/cm) initial surface-to-volume ratios, $(S/V)_0$, in the porous bed are sufficient to produce shock-induced detonation in the solid propellant. The thicker the porous bed, the smaller the required $(S/V)_0$ for detonation. For a fixed porous bed thickness there is a lower bound for $(S/V)_0$ for which detonation occurs. Near this lower bound the outcome is very sensitive to the initial $(S/V)_0$.

In the two dimensional 2DL calculations, Figs. 7a-8d, somewhat larger $(S/V)_0$ values (150 to 175/cm) produce detonation in the solid propellant. (Remember that 1-mm cubes have a (S/V) of 60/cm, so these $(S/V)_0$ values for detonation represent coarse material.) The change of initial ignition segment length from 0.8 to 2.4 cm makes a noticeable difference in the calculation and indicates that a segment of 5 to 10 cm would be essentially the one-dimensional case. For instance, one-dimensional calculation 4c, with a 2.6-cm-thick bed and $(S/V)_0$ = 120/cm, induces detonation in 25.3 μs; the two-dimensional calculation 8c, with a 2.6-cm-thick porous bed, a 2.4-cm initial ignition segment, and $(S/V)_0$ = 150/cm, induces detonation in 32.9 μs. However, the two-dimensional effect is pronounced in calculation 7a, where $(S/V)_0$ = 125/cm. In that situation a steady deflagration runs along the case and does not induce detonation. Rather, the calculation shows that a case burst is the likely result.

These calculations have shown that, with simple assumptions as to the burning of a porous bed and with shock-induced detonation modeled in the solid propellant, the motor detonations may occur without the necessity of a deflagration-to-detonation transition in the porous bed itself.

REFERENCES

1. Charles L. Mader and Milton Samuel Shaw, "User's Manual for SIN," Los Alamos Scientific Laboratory report LA-7264-M (September 1978).

2. Charles L. Mader, Numerical Modeling of Detonations, (University of California Press, 1979).

3. Charles L. Mader and Charles A. Forest, "Two-Dimensional Homogeneous and Heterogeneous Detonation Wave Propagation," Los Alamos Scientific Laboratory report LA-6259 (June 1976).

4. Charles A. Forest, "Burning and Detonation," Los Alamos Scientific Laboratory report LA-7245 (July 1978).

5. Charles L. Mader, "Detonation Properties of Condensed Explosives Computed Using the Becker-Kistiakowsky-Wilson Equation of State," Los Alamos Scientific Laboratory report LA-2900 (July 1963).

6. J. B. Ramsay and A. Popolato, "Analysis of Shock Wave and Initiation Data for Solid Explosives, Fourth Symposium on Detonation, ACR-126, 233 (1965).

7. Group M-3, LASL, 1976, unpublished data.

APPENDIX

FOREST FIRE CALCULATIONS

The Forest Fire shock-induced decomposition rates are calculated for VOP 7 at densities ρ_0 = 1.91, 1.719, and 1.528 g/cm^3. The ρ_0 = 1.91 case is based on wedge-test data on undamaged solid propellant. The ρ_0 = 1.719 and ρ_0 = 1.528 g/cm^3 cases are extrapolated from the ρ_0 = 1.91 g/cm^3 case using the method of Ref. 4.

In each case there are three sections. The first section lists the input data consisting of the "Pop-Plot line," the reaction Hugoniot, and the HOM equation-of-state constants. The second section lists, for each shock pressure, the distance to detonation (RUN), the various shock state variables, and the decomposition rate (RATE). The third section lists the coefficients for the polynomial fit of ℓn (RATE) and shows the fit agreement at the various pressure values. Definitions of listed variables are as follows:

RUN = distance to detonation (cm)

P = shock pressure (Mbar)

V = shock specific volume (cm^3/g)

UP = shock particle velocity (cm/μs)

US = shock velocity (cm/μs)

W = mass fraction of undecomposed propellant

RATE = -(1/W)(dW/dt) (1/μs)

TEMPERATURE = solid-product mixture temperature (K)

TIME = time to detonation (μs)

<u>ρ_0 = 1.91 g/cm^3</u>

```
 VOP-7    RHO=1.910, PCJ=0.3182, D=0.80927, VCJ=0.390375                SMAR79     RHO = 1.91000
POP PLOT, LN(RUN) = A1 + A2*LN(P-A3),  A1 = -5.299277E+00  A2 = -1.613201E+00  A3 =  0.
REACTION HUGONIOT,  US = C + S*UP,      C =  2.430000E-01   S =  2.500000E+00
CJ DETONATION PRESSURE =  3.182000E-01

HOM EQUATION OF STATE CONSTANTS
VOP-7 HOM CONSTANTS, MARCH 1976
UNREACTED EXPLOSIVE
 2.43000000000E-01 1.87900000000E+00 0.                 0.
 0.               -1.31440849979E+01-8.52022804920E+01-1.41271692413E+02
-9.96282582663E+01-2.35782395022E+01 1.50000000000E+00 3.30000000000E-01
 5.23560209424E-01 1.16965000000E-04 0.                 0.
 3.00000000000E+02 0.                0.                 0.
 0.                0.                0.
DETONATION PRODUCTS
-3.59225007104E+00-2.25139095825E+00 3.07083271071E-01-3.38388105816E-02
 3.26317134386E-04-1.56957579961E+00 5.63240444420E-01 9.14476859528E-02
 8.61048912339E-03 3.20340178818E-04 8.05038175417E+00-4.75298681101E-01
 1.00767476473E-01 5.25836857192E-03-4.21628859215E-03 5.00000000000E-01
 1.00000000000E-01
```

VOP-7 RHO=1.910, PCJ=0.3182, D=0.80927, VCJ=0.390375 5MAR79 RHO = 1.91000
POP PLOT, LN(RUN) = A1 + A2*LN(P-A3), A1 = -5.299277E+00 A2 = -1.613201E+00 A3 = 0.
REACTION HUGONIOT, US = C + S*UP, C = 2.430000E-01 S = 2.500000E+00

RUN	P	V	UP	US	W	RATE	TEMPERATURE	TIME
14.95696	.00700	.49840	.01327	.27618	.99878	4.5445E-04	332.91169	49.42350
12.05842	.00800	.49566	.01494	.28035	.99844	6.5349E-04	338.15229	39.00259
9.97175	.00900	.49306	.01657	.28442	.99808	9.0144E-04	343.49391	31.61047
8.41308	.01000	.49060	.01815	.28839	.99769	1.2030E-03	348.94603	26.16659
2.75000	.02000	.47128	.03233	.32384	.99256	8.1878E-03	409.83418	7.36095
1.42976	.03000	.45792	.04438	.35394	.98581	2.5956E-02	481.38143	3.43612
.89890	.04000	.44786	.05503	.38057	.97793	5.9905E-02	561.60396	1.98441
.62716	.05000	.43988	.06468	.40471	.96912	1.1607E-01	648.88071	1.29034
.46735	.06000	.43333	.07358	.42694	.95950	2.0135E-01	742.05991	.90525
.36445	.07000	.42781	.08187	.44767	.94914	3.2371E-01	840.32981	.66960
.29383	.08000	.42307	.08966	.46715	.93805	4.9237E-01	943.11187	.51501
.24298	.09000	.41894	.09704	.48559	.92626	7.1809E-01	1049.98967	.40817
.20500	.10000	.41528	.10406	.50314	.91375	1.0135E+00	1160.66309	.33129
.17578	.11000	.41202	.11077	.51992	.90050	1.3937E+00	1274.93225	.27414
.15276	.12000	.40908	.11721	.53602	.88648	1.8764E+00	1392.61735	.23051
.13426	.13000	.40641	.12341	.55152	.87165	2.4832E+00	1513.64836	.19646
.11913	.14000	.40397	.12939	.56648	.85596	3.2400E+00	1637.97808	.16939
.10658	.15000	.40173	.13518	.58095	.83936	4.1785E+00	1765.60019	.14751
.09604	.16000	.39967	.14079	.59498	.82177	5.3381E+00	1896.54647	.12958
.08710	.17000	.39775	.14624	.60861	.80312	6.7676E+00	2030.88591	.11471
.07942	.18000	.39597	.15155	.62186	.78331	8.4845E+00	2168.72565	.10223
.07279	.19000	.39431	.15671	.63478	.76223	1.0700E+01	2310.23771	.09167
.06701	.20000	.39275	.16175	.64737	.73975	1.3386E+01	2455.55443	.08265
.06194	.21000	.39128	.16667	.65967	.71571	1.6722E+01	2604.96896	.07489
.05746	.22000	.38990	.17148	.67170	.68993	2.0879E+01	2758.82306	.06816
.05348	.23000	.38859	.17619	.68347	.66222	2.6149E+01	2917.38565	.06229
.04993	.24000	.38736	.18080	.69500	.63224	3.2859E+01	3081.33284	.05715
.04675	.25000	.38619	.18532	.70630	.59975	4.1522E+01	3251.02040	.05260
.04389	.26000	.38507	.18975	.71738	.56429	5.2817E+01	3427.39277	.04858
.04129	.27000	.38401	.19411	.72827	.52528	6.8479E+01	3611.58182	.04499
.03894	.28000	.38300	.19838	.73896	.48206	9.0199E+01	3804.77699	.04178
.03680	.29000	.38204	.20259	.74947	.43367	1.2206E+02	4008.89938	.03890
.03484	.30000	.38111	.20672	.75980	.37856	1.7262E+02	4227.13523	.03631
.03304	.31000	.38023	.21079	.76998	.31469	2.6104E+02	4463.46245	.03396
.03139	.32000	.37938	.21480	.77999	.23827	4.4795E+02	4725.64909	.03183
.02987	.33000	.37857	.21874	.78986	.14185	1.0436E+03	5029.16661	.02989

VOP-7 RHO=1.910, PCJ=0.3182, D=0.80927, VCJ=0.390375 5MAR79 RHO = 1.91000
LN(RATE) = C(1) + C(2)*P + ... + C(M+1)*(P**M)
C(I=1,15) = -1.1388137087E+01 7.4244494753E+02 -3.9001043823E+04 1.4360231342E+06 -3.5485237838E+07
6.0353837716E+08 -7.2485568288E+09 6.2592155546E+10 -3.9223349711E+11 1.7835649392E+12
-5.8195013102E+12 1.3266461370E+13 -2.0047190526E+13 1.8032047764E+13 -7.3044357793E+12

PRESSURE	RATE	FIT	REL. ERROR
7.000000E-03	4.544536E-04	4.594973E-04	-.011098
8.000000E-03	6.534904E-04	6.511656E-04	.003557
9.000000E-03	9.014369E-04	8.946253E-04	.007556
1.000000E-02	1.202997E-03	1.195815E-03	.005970
2.000000E-02	8.187783E-03	8.306138E-03	-.014455
3.000000E-02	2.595608E-02	2.570882E-02	.009526
4.000000E-02	5.990513E-02	5.959579E-02	.005164
5.000000E-02	1.160661E-01	1.167772E-01	-.006127
6.000000E-02	2.013525E-01	2.025153E-01	-.005775
7.000000E-02	3.237140E-01	3.232286E-01	.001500
8.000000E-02	4.923715E-01	4.896281E-01	.005572
9.000000E-02	7.180935E-01	7.157400E-01	.003277
1.000000E-01	1.013540E+00	1.015304E+00	-.001740
1.100000E-01	1.393657E+00	1.399965E+00	-.004526
1.200000E-01	1.876387E+00	1.882210E+00	-.003103
1.300000E-01	2.483157E+00	2.481516E+00	.000661
1.400000E-01	3.239955E+00	3.228620E+00	.003498
1.500000E-01	4.178544E+00	4.164127E+00	.003450
1.600000E-01	5.338128E+00	5.332528E+00	.001049
1.700000E-01	6.767625E+00	6.777353E+00	-.001437
1.800000E-01	8.484549E+00	8.544936E+00	-.007117
1.900000E-01	1.069975E+01	1.070051E+01	-.000071
2.000000E-01	1.338585E+01	1.335101E+01	.002603
2.100000E-01	1.672151E+01	1.666106E+01	.003615
2.200000E-01	2.087868E+01	2.085101E+01	.001325
2.300000E-01	2.614905E+01	2.618110E+01	-.001226
2.400000E-01	3.285860E+01	3.295323E+01	-.002880
2.500000E-01	4.152215E+01	4.158946E+01	-.001621
2.600000E-01	5.281749E+01	5.284537E+01	-.000528
2.700000E-01	6.847879E+01	6.815557E+01	.004720
2.800000E-01	9.019909E+01	9.003786E+01	.001788
2.900000E-01	1.220646E+02	1.225872E+02	-.004281
3.000000E-01	1.726174E+02	1.730351E+02	-.002420
3.100000E-01	2.610386E+02	2.596577E+02	.005290
3.200000E-01	4.479529E+02	4.491115E+02	-.002586
3.300000E-01	1.043568E+03	1.043127E+03	.000422

$\rho_0 = 1.719$ g/cm^3

```
 VOP-7    RHO=1.719, PCJ=0.2547, D=0.74842, VCJ=0.427874          28SEP79     RHO = 1.71900
POP PLOT, LN(RUN) = A1 + A2*LN(P-A3),  A1 = -5.299277E+00  A2 = -1.613201E+00  A3 =  0.
REACTION HUGONIOT,  US = C + S*UP,      C =  2.430000E-01   S =  1.900000E+00
CJ DETONATION PRESSURE =  2.547000E-01

HOM EQUATION OF STATE CONSTANTS
 VOP-7   RHO=1.7190 = 0.90*1.91,  SOLID IS 1.91, GAS IS BKW FOR 1.7190
UNREACTED EXPLOSIVE
 2.43000000000E-01 1.87900000000E+00 0.                  0.
 0.               -1.31440849979E+01-8.52022804920E+01-1.41271692413E+02
-9.96282582663E+01-2.35782395022E+01 1.50000000000E+00 3.30000000000E-01
 5.23560209424E-01 1.16965000000E-04 0.                  0.
 3.00000000000E+02 0.                0.                  0.
 0.                0.                0.
DETONATION PRODUCTS
-3.48829964362E+00-2.21293918558E+00 2.84088396236E-01-3.45908309471E-02
 1.61341661461E-03-1.52769658343E+00 5.11751877215E-01 6.91391026790E-02
 5.09642892264E-03 1.40021106127E-04 8.14735025976E+00-4.29018154047E-01
 8.86488937040E-02-1.18036109477E-02 6.09785049038E-04 5.00000000000E-01
 1.00000000000E-01
```

```
 VOP-7    RHO=1.719, PCJ=0.2547, D=0.74842, VCJ=0.427874          28SEP79     RHO = 1.71900
POP PLOT, LN(RUN) = A1 + A2*LN(P-A3),  A1 = -5.299277E+00  A2 = -1.613201E+00  A3 =  0.
REACTION HUGONIOT,  US = C + S*UP,      C =  2.430000E-01   S =  1.900000E+00
```

RUN	P	V	UP	US	W	RATE	TEMPERATURE	TIME
7.78617	.00300	.51189	.01447	.12057	1.00000	6.7323E-04	316.61485	45.79475
6.15185	.00400	.50843	.01712	.13589	1.00000	1.0573E-03	322.35454	32.99259
5.05765	.00500	.50514	.01957	.14864	1.00000	1.5366E-03	327.89004	25.28078
4.27110	.00600	.50202	.02187	.15960	1.00000	2.1184E-03	333.25728	20.16817
3.67818	.00700	.49904	.02406	.16925	1.00000	2.8111E-03	338.48638	16.55762
3.21562	.00800	.49620	.02616	.17791	1.00000	3.6228E-03	343.60241	13.89029
2.84521	.00900	.49348	.02818	.18577	1.00000	4.5619E-03	348.62633	11.85180
2.54242	.01000	.49087	.03014	.19299	1.00000	5.6351E-03	353.57575	10.25197
1.13581	.02000	.46962	.04735	.24570	1.00000	2.5564E-02	401.33815	3.67531
.67376	.03000	.45411	.06188	.28204	1.00000	6.7948E-02	449.42619	1.90828
.45646	.04000	.44204	.07475	.31129	1.00000	1.4126E-01	499.47409	1.17227
.33438	.05000	.43224	.08646	.33644	1.00000	2.5445E-01	551.71344	.79419
.25796	.06000	.42406	.09727	.35885	1.00000	4.1699E-01	606.04662	.57390
.20647	.07000	.41707	.10736	.37929	1.00000	6.3910E-01	662.30753	.43417
.16987	.08000	.41099	.11687	.39820	.99783	9.3920E-01	733.56673	.33993
.14280	.09000	.40564	.12589	.41588	.99739	1.3188E+00	795.63285	.27334
.12211	.10000	.40087	.13448	.43256	.99692	1.7868E+00	859.30205	.22455
.10590	.11000	.39659	.14271	.44840	.99643	2.3724E+00	924.43891	.18772
.09293	.12000	.39270	.15061	.46350	.99591	3.0844E+00	990.96804	.15925
.08235	.13000	.38916	.15822	.47797	.99535	3.9405E+00	1058.80775	.13677
.07360	.14000	.38591	.16558	.49187	.99477	4.9592E+00	1127.88777	.11872
.06627	.15000	.38291	.17270	.50528	.99415	6.1617E+00	1198.1[illegible]414	.10401
.06006	.16000	.38013	.17960	.51824	.99349	7.5691E+00	1269.5[illegible]74	.09186
.05473	.17000	.37754	.18631	.53080	.99280	9.2076E+00	1341.98[illegible]73	.08172
.05014	.18000	.37513	.19284	.54299	.99207	1.1105E+01	1415.48034	.07315
.04614	.19000	.37287	.19921	.55484	.99129	1.3289E+01	1489.97812	.06586
.04263	.20000	.37074	.20542	.56638	.99047	1.5800E+01	1565.45404	.05960
.03953	.21000	.36874	.21149	.57763	.98961	1.8677E+01	1641.88012	.05419
.03678	.22000	.36684	.21743	.58861	.98868	2.1954E+01	1719.23522	.04947
.03433	.23000	.36505	.22324	.59935	.98770	2.5684E+01	1797.53841	.04534
.03213	.24000	.36335	.22893	.60985	.98666	2.9922E+01	1876.70559	.04171
.03015	.25000	.36174	.23452	.62014	.98555	3.4729E+01	1956.76174	.03849
.02837	.26000	.36020	.24000	.63022	.98437	4.0175E+01	2037.70130	.03563

```
 VOP-7    RHO=1.719, PCJ=0.2547, D=0.74842, VCJ=0.427874          28SEP79     RHO = 1.71900
LN(RATE) = C(1) + C(2)*P + ... + C(M+1)*(P**M)
C(I=1,15) =  -8.9326669951E+00  6.7032084478E+02 -4.6607471632E+04  2.3710194210E+06 -8.0551210509E+07
              1.8618617437E+09 -3.0065099958E+10  3.4604180178E+11 -2.8708003619E+12  1.7191694313E+13
             -7.3575459944E+13  2.1931732208E+14 -4.3232755531E+14  5.0637001735E+14 -2.6674552100E+14
```

PRESSURE	RATE	FIT	REL. ERROR
3.000000E-03	6.732275E-04	6.869510E-04	-.020385
4.000000E-03	1.057291E-03	1.044528E-03	.012072
5.000000E-03	1.536559E-03	1.511214E-03	.016495
6.000000E-03	2.118365E-03	2.096056E-03	.010531
7.000000E-03	2.811118E-03	2.805126E-03	.002131
8.000000E-03	3.622792E-03	3.642277E-03	-.005378
9.000000E-03	4.561904E-03	4.610095E-03	-.010564
1.000000E-02	5.635050E-03	5.710849E-03	-.013451
2.000000E-02	2.556390E-02	2.527466E-02	.011314
3.000000E-02	6.794815E-02	6.788530E-02	.000925
4.000000E-02	1.412611E-01	1.425637E-01	-.009221
5.000000E-02	2.544472E-01	2.540979E-01	.001373
6.000000E-02	4.169880E-01	4.139827E-01	.007207
7.000000E-02	6.391017E-01	6.397296E-01	-.000983
8.000000E-02	9.391999E-01	9.420487E-01	-.003033
9.000000E-02	1.318753E+00	1.322246E+00	-.002649
1.000000E-01	1.786764E+00	1.787180E+00	-.000233
1.100000E-01	2.372356E+00	2.361375E+00	.004629
1.200000E-01	3.084435E+00	3.076982E+00	.002416
1.300000E-01	3.940530E+00	3.951258E+00	-.002723
1.400000E-01	4.959235E+00	4.979987E+00	-.004185
1.500000E-01	6.161652E+00	6.163545E+00	-.000307
1.600000E-01	7.569067E+00	7.540780E+00	.003737
1.700000E-01	9.207605E+00	9.181191E+00	.002869
1.800000E-01	1.110491E+01	1.112582E+01	-.001884
1.900000E-01	1.328896E+01	1.334330E+01	-.004089
2.000000E-01	1.579998E+01	1.579734E+01	.000167
2.100000E-01	1.867683E+01	1.859449E+01	.004409
2.200000E-01	2.195375E+01	2.195145E+01	.000105
2.300000E-01	2.568402E+01	2.581337E+01	-.005036
2.400000E-01	2.992189E+01	2.979988E+01	.004077
2.500000E-01	3.472890E+01	3.477648E+01	-.001370
2.600000E-01	4.017505E+01	4.016804E+01	.000174

$\rho_0 = 1.528\ g/cm^3$

```
 VOP-7    RHO=1.528, PCJ=0.2025, D=0.69214, VCJ=0.473388          28SEP79     RHO = 1.52800

POP PLOT, LN(RUN) = A1 + A2*LN(P-A3),  A1 = -5.299277E+00  A2 = -1.613201E+00  A3 =  0.

REACTION HUGONIOT,  US = C + S*UP,      C =  2.430000E-01   S =  1.900000E+00

CJ DETONATION PRESSURE =  2.025000E-01

HOM EQUATION OF STATE CONSTANTS
 VOP-7   RHO=1.5280 = 0.80*1.91,  SOLID IS 1.91, GAS IS BKW FOR 1.5280
UNREACTED EXPLOSIVE
 2.43000000000E-01 1.87900000000E+00 0.                 0.
 0.               -1.31440849979E+01-8.52022804920E+01-1.41271692413E+02
-9.96282582663E+01-2.35782395022E+01 1.50000000000E+00 3.30000000000E-01
 5.23560209424E-01 1.16965000000E-04 0.                 0.
 3.00000000000E+02 0.                0.                 0.
 0.                0.                0.
DETONATION PRODUCTS
-3.39541732792E+00-2.17855054878E+00 2.62880541967E-01-3.03177017812E-02
 1.32748074892E-03-1.47397848981E+00 5.00459275865E-01 6.67841735386E-02
 4.90140589271E-03 1.34141177621E-04 8.24332651897E+00-4.04154640448E-01
 7.03634211072E-02-8.32073192325E-03 3.89970358806E-04 5.00000000000E-01
 1.00000000000E-01
```

VOP-7 RHO=1.528, PCJ=0.2025, D=0.69214, VCJ=0.473388 28SEP79 RHO = 1.52800
POP PLOT, LN(RUN) = A1 + A2*LN(P-A3), A1 = -5.299277E+00 A2 = -1.613201E+00 A3 = 0.
REACTION HUGONIOT, US = C + S*UP, C = 2.430000E-01 S = 1.900000E+00

RUN	P	V	UP	US	W	RATE	TEMPERATURE	TIME
6.64787	.00100	.51990	.01160	.05642	1.00000	5.8345E-04	306.47899	69.77571
4.36372	.00200	.51644	.01661	.07878	1.00000	1.2881E-03	315.00300	35.01640
3.31173	.00300	.51317	.02059	.09537	1.00000	2.1723E-03	323.29906	22.81552
2.67968	.00400	.51006	.02403	.10893	1.00000	3.2525E-03	331.40694	16.59690
2.25040	.00500	.50711	.02714	.12056	1.00000	4.5408E-03	339.35963	12.84435
1.93711	.00600	.50429	.03002	.13082	1.00000	6.0509E-03	347.18467	10.34677
1.69733	.00700	.50161	.03271	.14006	1.00000	7.7956E-03	354.90513	8.57382
1.50747	.00800	.49903	.03526	.14848	1.00000	9.7878E-03	362.54037	7.25631
1.35321	.00900	.49657	.03770	.15626	1.00000	1.2041E-02	370.10674	6.24308
1.22536	.01000	.49421	.04003	.16349	1.00000	1.4566E-02	377.61805	5.44278
.59988	.02000	.47477	.05995	.21834	1.00000	5.7704E-02	451.59258	2.06662
.37500	.03000	.46045	.07629	.25736	1.00000	1.4265E-01	526.33504	1.11097
.26301	.04000	.44924	.09060	.28894	1.00000	2.8321E-01	603.20177	.69869
.19754	.05000	.44010	.10353	.31608	1.00000	4.9395E-01	682.36367	.48151
.15532	.06000	.43243	.11542	.34022	1.00000	7.9047E-01	763.69966	.35254
.12621	.07000	.42587	.12649	.36216	1.00000	1.1895E+00	847.02591	.26950
.10513	.08000	.42015	.13691	.38242	1.00000	1.7092E+00	932.16047	.21282
.08929	.09000	.41511	.14677	.40132	1.00000	2.3688E+00	1018.94009	.17236
.07704	.10000	.41061	.15615	.41910	1.00000	3.1898E+00	1107.22311	.14246
.06733	.11000	.40656	.16513	.43595	1.00000	4.1952E+00	1196.88670	.11973
.05948	.12000	.40288	.17375	.45200	1.00000	5.4103E+00	1287.82489	.10204
.05303	.13000	.39953	.18204	.46735	1.00000	6.8625E+00	1379.94556	.08800
.04765	.14000	.39645	.19005	.48209	1.00000	8.5821E+00	1473.16805	.07666
.04311	.15000	.39360	.19781	.49628	1.00000	1.0602E+01	1567.42128	.06739
.03924	.16000	.39096	.20532	.50999	1.00000	1.2960E+01	1662.64221	.05969
.03591	.17000	.38851	.21263	.52325	.99477	1.5888E+01	1785.19644	.05324
.03302	.18000	.38621	.21973	.53611	.99424	1.9115E+01	1884.33980	.04778
.03049	.19000	.38406	.22666	.54861	.99368	2.2831E+01	1984.36566	.04312
.02826	.20000	.38204	.23341	.56077	.99309	2.7098E+01	2085.26108	.03910
.02629	.21000	.38014	.24001	.57262	.99246	3.1984E+01	2186.94607	.03562

VOP-7 RHO=1.528, PCJ=0.2025, D=0.69214, VCJ=0.473388 28SEP79 RHO = 1.52800
LN(RATE) = C(1) + C(2)*P + ... + C(M+1)*(P**M)
C(I=1,15) = -8.2368054082E+00 9.4571613285E+02 -1.0706726255E+05 8.1291429969E+06 -3.8835989179E+08
1.2184228166E+10 -2.6132894529E+11 3.9396099761E+12 -4.2403606950E+13 3.2723664429E+14
-1.7957736260E+15 6.8376677648E+15 -1.7165541233E+16 2.5542660234E+16 -1.7059908589E+16

PRESSURE	RATE	FIT	REL. ERROR
1.000000E-03	5.834475E-04	6.171467E-04	-.057759
2.000000E-03	1.288078E-03	1.213254E-03	.058089
3.000000E-03	2.172341E-03	2.086110E-03	.039695
4.000000E-03	3.252515E-03	3.231839E-03	.006357
5.000000E-03	4.540783E-03	4.620723E-03	-.017605
6.000000E-03	6.050893E-03	6.215166E-03	-.027149
7.000000E-03	7.795626E-03	7.984952E-03	-.024286
8.000000E-03	9.787774E-03	9.915635E-03	-.013063
9.000000E-03	1.204141E-02	1.201057E-02	.002562
1.000000E-02	1.456641E-02	1.428898E-02	.019046
2.000000E-02	5.770363E-02	5.603987E-02	.028833
3.000000E-02	1.426539E-01	1.478901E-01	-.036706
4.000000E-02	2.832071E-01	2.804847E-01	.009613
5.000000E-02	4.939484E-01	4.836030E-01	.020944
6.000000E-02	7.904688E-01	8.003056E-01	-.012444
7.000000E-02	1.189516E+00	1.208818E+00	-.016227
8.000000E-02	1.709153E+00	1.693027E+00	.009435
9.000000E-02	2.368752E+00	2.333351E+00	.014945
1.000000E-01	3.189795E+00	3.207632E+00	-.005592
1.100000E-01	4.195243E+00	4.257653E+00	-.014877
1.200000E-01	5.410292E+00	5.398721E+00	.002139
1.300000E-01	6.862506E+00	6.765338E+00	.014159
1.400000E-01	8.582110E+00	8.585824E+00	-.000433
1.500000E-01	1.060233E+01	1.074935E+01	-.013867
1.600000E-01	1.295983E+01	1.294456E+01	.001178
1.700000E-01	1.588774E+01	1.562635E+01	.016452
1.800000E-01	1.911481E+01	1.945068E+01	-.017571
1.900000E-01	2.283069E+01	2.264019E+01	.008344
2.000000E-01	2.709809E+01	2.715400E+01	-.002063
2.100000E-01	3.198407E+01	3.197739E+01	.000209

Printed in the United States of America. Available from
National Technical Information Service
US Department of Commerce
5285 Port Royal Road
Springfield, VA 22161

Microfiche $3.00

001-025	4.00	126-150	7.25	251-275	10.75	376-400	13.00	501-525	15.25
026-050	4.50	151-175	8.00	276-300	11.00	401-425	13.25	526-550	15.50
051-075	5.25	176-200	9.00	301-325	11.75	426-450	14.00	551-575	16.25
076-100	6.00	201-225	9.25	326-350	12.00	451-475	14.50	576-600	16.50
101-125	6.50	226-250	9.50	351-375	12.50	476-500	15.00	601-up	

Note: Add $2.50 for each additional 100-page increment from 601 pages up.